Estimation of Load Inertia using Ambient Measurements from Synchrophasor Technology

Marina Elenkova, Markos Asprou, Lenos Hadjidemetriou and Christos G. Panayiotou
KIOS Research and Innovation Center of Excellence
Department of Electrical and Computer Engineering
Nicosia, Cyprus
e-mail: {elenkova.marina, asprou.markos, hadjidemetriou.lenos, christosp}@ucy.ac.cy

***Abstract*—The number of non-synchronous renewables and dynamic loads is rapidly increasing, which results in a variable system inertia. Thus, accurately quantifying the contribution of the demand side to the system inertia is becoming an important aspect and can help operators to maintain the system stability. This paper proposes an online estimation method to monitor the time-varying inertia of the loads under normal operating conditions. The widely used composite load model (CLM) of Western Electricity Coordinating Council (WECC) is employed, capable of representing diverse composition and dynamic characteristics of loads, in an aggregate manner. A measurement-oriented approach is proposed to estimate the load inertia considering only ambient measurements provided by Phasor Measurement Units (PMUs) during normal grid operation. The inertia estimation of load buses at the transmission level is performed using the Least Squares (LS) method. The proposed method is validated under various case studies using the 39-bus test system, where the CLM is integrated. The case studies consider scenarios with different load composition and time varying load inertia, demonstrating that the proposed method can accurately and dynamically estimate the load inertia by using only ambient PMU measurements.**

Keywords—Composite load model, Least Squares (LS), load inertia estimation, phasor measurement units (PMUs).

I. INTRODUCTION

The increasing penetration of Renewable Energy Sources (RESs) imposes various challenges to the secure and stable operation of power systems. A significant part of the system inertia relies on the physical inertia of the rotating mass of conventional synchronous generators. Therefore, when conventional generation plants are replaced by non-rotating RES (e.g., photovoltaics), the system inertia is reduced threatening the system stability. Even in case of rotating RES (e.g., wind power systems), the integration through power electronics converter decouples the physical inertia of wind turbines neglecting their contribution to system inertia. As a result, the green transition of power systems reduces the inertia introduced by the generation side, leading to low-inertia grids. In such grids, system frequency becomes very sensitive to generation-load unbalances and maintaining the frequency stability is a crucial aspect for the system operators [1], [2].

A considerable amount of inertia is available from the demand side with potentially important economic savings to the system [3]. The cost reduction can be achieved by optimizing the unit commitment problem that includes also ancillary services and demand inertia. In this case, the inertia requirements for frequency stability are partially satisfied by the demand inertia instead of committing conventional units. Thus, the system operational cost is reduced as less generators are needed online. Industry sector is also expressing interest in real-time estimation and forecasting of the effective (system) inertia [4], which is a combination of physical inertia from rotating synchronous generation, controlled responses of power electronic converters (virtual inertia by RES [2]), and passive responses from domestic and industrial demand.

From a system operator perspective, an online awareness of the inertia provided by different contributors to an area or to the system inertia can be useful, especially in case of a contingency. However, the large number of diverse load components, the time-varying and weather-dependent compositions, and the lack of detailed load information and measurements, makes the estimation of the load inertia difficult. As the number of PMUs installed in power systems is constantly growing, monitoring of load inertia online and in real-time may become feasible. Consequently the situational awareness of the power system operators will be enhanced considerably.

Most of the relevant research focuses on quantifying the available inertia provided by the generation side or estimating the effective system inertia, and limited work has been done to estimate the demand side inertia. In this context, early approaches [5], [6] use the swing equation to estimate the system inertia during large disturbance events, where the contribution of generation, demand and virtual inertia through RES is aggregated. A measurement-based approach has been recently proposed [7], [8] for estimating the effective inertia of different areas in multiarea interconnected power systems. In [7] a relationship between effective area inertia and area demand in MW is derived. However, the method is event-based and can only estimate inertia after a severe disturbance. In [8], the application of the presented method to real measurement data, revealed that the estimated area inertia is larger than the expected theoretical value. One of the reasons was that the area under study contains large industrial load centers with motors that can contribute to the effective inertia.

In [9], [10] and [11] the effective inertia is estimated under normal operating conditions using ambient data in the estimation process. However, in these methods, the aggregation reflects the system inertia, without estimating the contribution of generation and demand side individually. Knowledge of the inertia at a certain load bus could benefit the system operators regarding the load shedding schemes that are applied. Prioritizing the load buses contributing to the effective inertia as higher priority loads and thus avoid rejecting those buses during a contingency could help in preventing total blackouts and cascading events.

An early effort to distinguish the demand inertia contribution is reported in [12]. In the aforementioned approach, the load inertia of the Irish Power System is calculated using a white-box method, utilizing post event data.

This work was supported in part by the European Regional Development Fund and the Republic of Cyprus through the Research and Innovation Foundation under Project: INTEGRATED/0916/0035 – EMPOWER; in part by the European Union's Horizon 2020 Research and Innovation Programme under grant agreement No 957739 (OneNet); and in part by the European Union's Horizon 2020 research and innovation programme under grant agreement N0 739551 (KIOS CoE – TEAMING) and from the Republic of Cyprus through the Deputy Ministry of Research, Innovation and Digital Policy.

The load inertia is extracted from the system overall inertia by subtracting the contribution from the synchronous generators and the embedded generation. Similarly, in [13], [14] the demand side inertia contribution of the Great Britain Power System was estimated from recorded grid frequency during an outage events. It was found that an average of 20% of the system inertia is provided from the demand side [14], highlighting that the amount of demand inertia available is significant. In [15], the load inertia provided by different power consumer groups is estimated, analyzing a permanent short circuit event. In [16], the inertia contribution from power station auxiliary loads is also taken into consideration in the overall system inertia using measurements taken during HVDC power perturbations. However, the disturbance-based estimation methods allow inertia estimation after severe events which do not occur very often in a power system and thus the real-time inertia estimation is not feasible.

The main contribution of this paper is the development of a novel methodology that can estimate and track the time-varying load inertia of a bus using only ambient PMU measurements. The proposed method is applied to load buses with adequate load inertia that can contribute significantly to the system inertia. The aggregated load inertia is estimated online, under normal operation, without the necessity of a disturbance to occur, as opposed to the disturbance-based estimation methods proposed in literature. Furthermore, the reduced data length used for the estimation process allows a near real-time estimation. Lastly, the estimation scheme relies only on frequency and power measurements at the system bus while knowledge of any other data is not required (e.g. contribution from synchronous generator units to the system inertia, embedded generation).

The remainder of the paper is organized as follows: The composite load model that is used in this study to represent the loads of a power system is described in Section II. Section III presents the proposed load inertia estimation scheme. The case studies and the results are presented and discussed in Section IV and the paper concludes in Section V.

II. WECC Composite Load Model

Load modelling is essential for power system stability analysis, planning and control. Due to the diversity of load types and the integration of distributed energy resources (DERs), WECC has developed a composite load model to accurately represent a variety of load compositions, as shown in Fig. 1. More specifically, the model includes a substation transformer, shunt capacitor, and a feeder equivalent. The load model, which is attached at low voltage side, consists of three induction three-phase motor models with different dynamic characteristics (Motors A-C), one single-phase motor model (Motor D), an electronic load, a static load and a distributed generator model (DER).

The motor models represent the aggregation of many motors throughout the distribution system, with the same characteristics. Motor A represents the aggregation of three-phase induction motors with relatively low inertia, driving constant torque loads, such as commercial and industrial air-conditioning compressors, positive displacement pumps, etc. Motor B represents the three-phase induction motors with high inertia, driving variable torque loads whose torque is proportional to the square of mechanical speed. Typical loads of this category are commercial ventilation fans and air handling systems. Motor C represents the three-phase induction motors with relatively low inertia, driving loads whose torque is proportional to the square of speed, e.g.

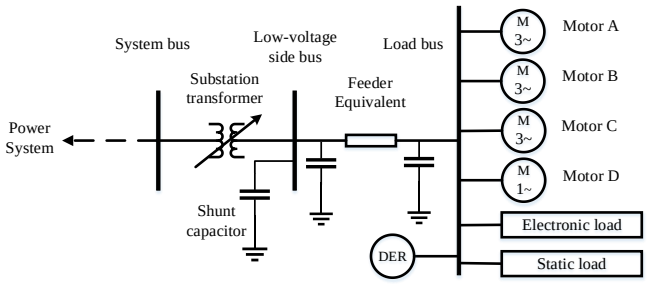

Fig. 1. Schematic diagram - WECC Composite Load Model

centrifugal pumps. Motor D is a performance based model of single-phase residential heat ventilation and air-conditioning (HVAC) system. The model represents many individual single-phase A/C compressors and their protective devices. Motor A-C consider the equivalent circuit of a three-phase induction motor and Motor D follows the single-phase motor circuit. In motors A-C, the dynamic response relies on [17]:

$$\frac{d\omega}{dt} = \frac{T_e - T_m}{2H} \tag{1}$$

where ω is the rotor speed, T_e is the electromagnetic torque, T_m is the mechanical input torque, and H is the inertia constant (in sec). The torque characteristics of the mechanical input torque T_m is calculated as follows:

$$T_m = T_{m0}\omega^{E_{trq}} \tag{2}$$

In (2), T_{m0} is the initial mechanical input torque and E_{trq} is the speed exponent for mechanical torque. Hence, for constant torque loads that are not dependent on motor speed the parameter E_{trq} is 0, while for speed dependent loads E_{trq} defines the type of dependency. The CLM also includes an electronic load and a static load model. The power electronic load component of the model represents the consumer loads that are connected to the system through an inverter-based interface, e.g. variable speed drive interfaced motor loads and consumer electronic devices. The active and reactive power output of the electronic model is given by a conditional linear function of the bus terminal voltage V_t [18]. In this way, the under-voltage operation of these devices is represented.

The static load represents all the loads that are not included by the previous models in the system, such as resistive heating loads and non-led based lighting loads. The model is represented by a polynomial representation that captures the active and reactive power sensitivity to voltage and frequency [17]. The share of each of the aforementioned components (motors, electronic and static loads) contributing to the total load can be specified by the user. Further information regarding the WECC CLM can be found in [17] and [18]. In [18] a detailed mathematical representation of the DER model which is not used in this study is also available.

III. Proposed Estimation Framework

In this section, the proposed estimation scheme for online monitoring of the load inertia at each bus is presented. The procedure consists of the following three steps, as depicted also in Fig. 2:

1) Data acquisition and preprocessing of frequency and power measurements used for the inertia estimation.
2) Load inertia estimation at a substation level using the LS method, considering an aggregated load representation.
3) Application of a smoothing technique on the estimated values to reduce the impact of erroneous estimations (outliers).

1) Data Preprocessing

Data preprocessing is employed to remove the measurement noise and to ensure estimation accuracy. First, frequency and power ambient measurements (during normal operating conditions) are collected from the system bus and converted in p.u. values. Next, the linear trend is removed and the measurements are filtered through a non-casual low-pass Butterworth filter to attenuate the higher frequency components. Then, the vectors that contain the difference between two consecutive values are constructed and used at the estimation stage, instead of the measured values, which is a common preprocessing technique. In this way, the part of the signal that is the same between adjacent measurements is removed.

2) Load Inertia Estimation using LS method

The LS is a method used for estimating the parameters of a model by finding a solution that minimizes the sum of the squared errors between the observed data and their estimated values. The form of the model is given by,

$$\mathbf{Y} = \mathbf{X}^{\mathrm{T}}\boldsymbol{\theta} \tag{3}$$

where $\mathbf{Y} \in R^{m\times 1}$ is the observation vector; $\mathbf{X} \in R^{m\times p}$ is the regressor matrix of m observations on p variables to be estimated; and $\boldsymbol{\theta} \in R^{p\times 1}$ is the vector of unknown parameters. The LS method aims to find the solution $\widehat{\boldsymbol{\theta}}_{\boldsymbol{LS}} = [\widehat{\theta}_1,\ \widehat{\theta}_2, \dots, \widehat{\theta}_p]^{\mathrm{T}}$ according to (4),

$$\widehat{\boldsymbol{\theta}}_{\boldsymbol{LS}} = \arg\min_{\boldsymbol{\theta}} \left\|\mathbf{Y} - \mathbf{X}^{\mathrm{T}}\widehat{\boldsymbol{\theta}}\right\|_2 = (\mathbf{X}^{\mathrm{T}}\mathbf{X})^{-1}\mathbf{X}^{\mathrm{T}}\mathbf{Y} \tag{4}$$

where $\|.\|_2$ denotes the Euclidian vector norm. In the proposed load inertia estimation scheme, a simplified model is considered, where all motors are lumped into one single fictitious motor. The dynamics of the aggregated motor model are given in p.u. by expressing (1) in steady state, using the torque-power relationship ($P = T\omega$) and $\omega \simeq 1$ p.u for steady state conditions. In the following linearized equation, the frequency (f) is used to approximate the rotor angle (ω) and the torque is converted into power (P),

$$\Delta P = 2H_D * \frac{d(\Delta f)}{dt} + D * \Delta f \tag{5}$$

where H_D is the aggregated inertia provided by the demand side and D represents the aggregated frequency-dependent term of (2). The simplified model is in the least squares format; the observation vector $\mathbf{Y} = [P_1 \dots P_m]^{\boldsymbol{T}}$ contains the power measurements P for m recorded samples; the vector $\Delta\mathbf{f} = [\Delta f_1 \dots \Delta f_m]^{\boldsymbol{T}}$ contains the frequency deviation Δf; the regressor matrix is $\mathbf{X} = [d(\Delta\mathbf{f})/dt\ \ \Delta\mathbf{f}]^{\mathrm{T}} \in \mathrm{R}^{2\times m}$, where $d(\Delta\mathbf{f})/dt$ is the one-dimensional numerical gradient of the vector $\Delta\mathbf{f}$. The aggregated load inertia H_D is estimated by solving the LS problem $\widehat{\boldsymbol{\theta}}_{\boldsymbol{LS}} = [\widehat{\theta}_1\ \widehat{\theta}_2]^{\mathrm{T}}$ and the load inertia can be extracted by the first element of the LS solution. Hence, the estimated load inertia value for estimation k is $H_{\mathrm{est,k}} = \widehat{\theta}_1/2$, using an estimation window of m measurements.

3) Data Smoothing

The discrete low-pass filter is applied on the estimation windows comprised of m measurements to smooth any erroneous estimations that can be considered as outliers, enhancing the estimation accuracy. The discrete low-pass filter used is in the following form,

$$H_{\mathrm{LP,k}} = \alpha H_{\mathrm{est,k}} + (1-\alpha)H_{\mathrm{LP,k-1}} \tag{6}$$

where $H_{\mathrm{LP,k}}$ and $H_{\mathrm{LP},k-1}$ are the smoothing values of the discrete low-pass filter (filter output) at estimation k and k-1, respectively; $H_{est,k}$ is the LS estimated load inertia of estimation k (filter input); and α is a smoothing constant with values ranging from 0 to 1.

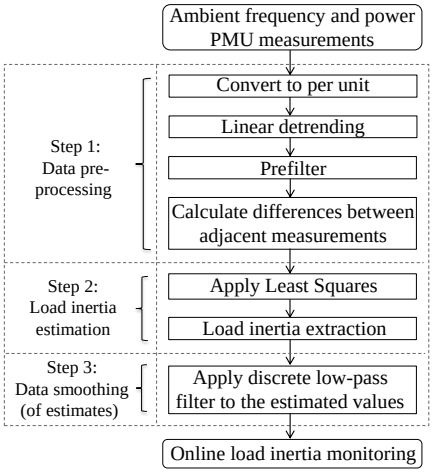

Fig. 2. Flowchart of load inertia estimation scheme

IV. Case Studies

The performance of the proposed method is tested using the IEEE 39-bus test system [19], modeled in DIgSILENT PowerFactory 2021 SP1. The IEEE 39-bus test system contains 10 generators (G_1-G_{10}) and 19 loads that change dynamically in time in order to mimic ambient load variations under normal operation. The load variations that are incorporated in the test system result in realistic ambient frequency variations within the range [49.9-50.1] Hz for system frequency 50 Hz. In the simulation, the droop constants of the generators are set to $R_{2\text{-}8}$ = 0.035 p.u., R_9 = 0.0338 p.u. and R_{10} = 0.05 p.u.; and the base power of G_1 is set to $S_{\mathrm{base},1}$ = 1200 MVA. The IEEE 39-bus test system has also been modified to include 3 additional generators connected in parallel to the existing generators G_5, G_7 and G_9 at the same bus. The rest of the system parameters are taken from [19]. The WECC Composite Load Model is incorporated at the IEEE 39-bus test system via a transformer at Bus 12, connecting a 20 MW load. The load connected at Bus 7 (Load 7 of [19]) is reduced by 20 MW to compensate the additional load of the CLM. The time domain simulation is performed with time step 0.001 sec, while frequency and power measurements at the system bus are recorded and sent to a Matlab script for the estimation stage every 0.2 sec. In Section IV.A the fraction of each CLM component varies and the load inertia is kept constant. In Section IV.B the estimation scheme is tested under time-varying load inertia, while the fraction of each component is kept constant. The rest of the CLM parameters are the default DigSilent values.

A. Constant load inertia

In this section, different compositions of load are used to evaluate the efficiency of the proposed estimation scheme. The load composition for each case study is presented in Table I for Motors A-C, the electronic load and the static load. The mean error (%) and maximum error (%) are selected as key performance indicators (KPIs). In this case, the percentage of the estimation error is calculated as follows:

$$Error\ (\%) = \left(\frac{H_{\mathrm{LP,k}} - H_{\mathrm{D,true}}}{H_{\mathrm{D,true}}}\right) \times 100\% \tag{7}$$

where $H_{LP,k}$ denotes the smoothed estimation result obtained using (6) at time step k and $H_{\mathrm{D,true}}$ is the true total load inertia,

TABLE I
CASES OF WECC COMPOSITE LOAD MODEL CONFIGURATION

Case	Load composition (%)						Mean Error (%)	Max Error (%)
	A	B	C	D	Elec.	Static		
1	97	1	1	1	0	0	1.29	3.79
2	1	97	1	1	0	0	2.03	4.73
3	1	1	97	1	0	0	1.69	4.72
4	85	5	5	5	0	0	1.51	5.07
5	10	70	10	10	0	0	1.81	4.34
6	20	20	40	20	0	0	1.60	4.42
7	33.3	33.3	33.3	0	0	0	2.28	5.08
8	26.6	26.6	26.6	0	10	10	3.95	7.74
9	20	20	20	0	20	20	6.09	9.48
10	13.3	13.3	13.3	0	30	30	2.00	5.67
11	15	25	30	10	15	5	2.91	5.91
12	25	35	30	0	10	0	1.40	2.84

as set in the simulation stage. The total load inertia that is comprised of Motors A-D is calculated as:

$$H_{D,true} = \frac{\sum_{i=1}^{n} H_i S_{B,i}}{\sum_{i=1}^{n} S_{B,i}} \quad (8)$$

In (8), H_i is the inertia of motor i, $S_{B,i}$ is the rated power of motor i and n is the total number of motors connected at the particular bus that contribute to the system load. In this study, i represents Motors A-D. The value of $H_{D,true}$ is used as an evaluation indicator for the accuracy of the proposed method after the estimation process. The results for 12 representative case studies are presented in Table I. The data window used for the estimation process is comprised of measurements that correspond to 15 sec with sampling time 0.2 sec. The total number of estimations performed for each case study corresponds to 30 min monitoring of frequency and power measurements at the system bus. For each estimation window, steps 1-3 are employed sequentially as described in Section III. In Step 1, the summation of the rated powers of the CLM components is used to convert in per unit. However, the system base value can be chosen arbitrarily. In this case, the true value of inertia $H_{D,true}$ is converted in p.u. of the new system base to evaluate the estimation accuracy. Furthermore, in Step 1, a 10th-order non-casual Butterworth filter with cut-off frequency f_c = 1 Hz is used in this study. The LS parameter estimation is then employed as described in Step 2. Table I presents the mean and maximum error results for a smoothing value of $\alpha = 0.05$ using (6) as shown in Step 3, while the estimation errors are calculated using (7) and (8). In (8) the value of inertia for Motor D is zero, as there is no contribution.

During the simulations presented in this section, the inertia of motors A-C is constant and given the same value for all case studies. Specifically, for Motor A the inertia is set as $H_A = 0.3$ sec (low-inertia model); for Motor B as $H_B = 0.8$ sec (high-inertia model); and for Motor C as $H_C = 0.2$ sec (low-inertia model). Then, simulations for various load compositions are performed. First, high fraction of one of the motors is considered (e.g. Cases 1-3) and then the fraction is decreased, while the fraction of the other motors increases accordingly (e.g. Cases 4-6). Electronic and static loads are also introduced as case studies. Starting with equal fraction of all 3 motors and non-existent electronic/static load (Case 7), the fraction of electronic and static loads is increased as presented in Table I (Cases 8-10). However, further increase in the percentage of loads with no inertia results in reducing the amount of load

TABLE II
TIME-VARYING LOAD INERTIA SCENARIO

	Inertia of motors (sec)			Total load inertia (sec)
	H_A	H_B	H_C	$H_{D,true}$
Stage 1	0.3	0.6	0.25	0.4
Stage 2	0.5	1.1	0.4	0.7
Stage 3	0.35	1	0.35	0.6

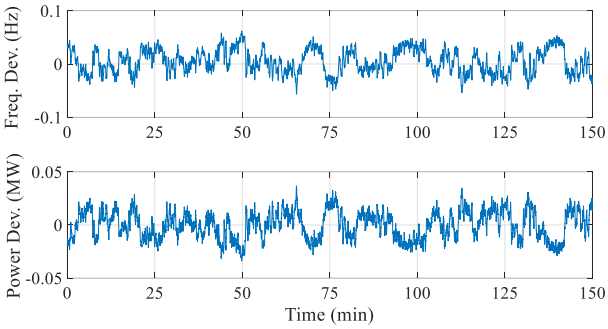

Fig. 3. Case 12: Frequency deviation (Hz) and Power deviation (MW)

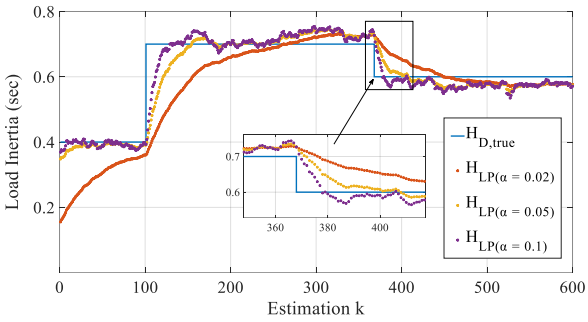

Fig. 4. Load inertia tracking

inertia that contribute to the system inertia. For instance, the amount of inertia provided by the generators is 29.201 GVA seconds for the 39-bus test system and in Case 7, where the load is comprised only from motors, the load inertia is 11.6 MVA seconds of inertia (0.05% of inertia provided by generators). Considering 2% share of each motor A-C results in approximately 0.7 MVA seconds of inertia (0.002% of the inertia provided by the generators) and thus the amount of load inertia is reduced. Therefore, the methodology is applied to load buses that can contribute to the system inertia.

Case studies with various load compositions were simulated resulting in general to low mean estimation error and maximum estimation error below 10% (e.g. Cases 11-12). As it can be seen in Table I, the case with the maximum mean error is Case 9 with 6.09% mean error and maximum error 9.48%. The performance of the estimation scheme to the rest of the case studies that are not shown is similar (low mean error and maximum error below 10%). Hence, it was verified that the algorithm is capable of estimating the load inertia for different load composition scenarios with accuracy. Moreover, as the computation time for each individual estimation is approximately 0.03 sec, the results are instantly available which is crucial for near real-time applications for load inertia estimation.

B. Time-varying load inertia

In this section a time-varying load inertia case is presented and the feasibility of the proposed estimation scheme to

monitor the load inertia is verified. Case study 12 of Table I is simulated with constant fractions of the CLM components, while the load inertia varies. Three stages of load inertia changes are presented, as shown in Table II. First, the transition from Stage 1 to Stage 2 consists of a large inertia increase for all loads (Motors A-C). The change in Motor B is chosen to be larger than the rest of the motors, as Motor B represents loads with large inertia value. Next, in Stage 3, there is a small decrease in inertia for all load components. The value of the total load inertia $H_{D,true}$ given in Table II is calculated using (8). In Fig. 3, the frequency deviation (Hz) from the nominal frequency and the power deviation (MW) from the nominal load for the simulated case study are given for illustration purposes. Considering a data monitoring length of 150 min as illustrated in Fig. 4, the total load inertia remains at 0.4 sec during the first 25 min, then changes to 0.7 sec from 25 to 92 min, while from 92 to 150 min the inertia changes to 0.6 sec. As it can be observed in Fig. 3, the proposed method can properly capture the change of the inertia value considering only ambient measurements (normal operating conditions), while no disturbance occurs during this case study. The results of the load inertia estimation in case that the inertia of the load is changing are shown in Fig. 4.

Different values of the smoothing constant α are also presented in Fig. 4. Specifically, the constant α of the discrete low-pass filter is given a small value (α = 0.02) and then increased (α = 0.05 and α = 0.1). As it can be seen in Fig. 4, choosing a small value of α may result in attenuating any possible outliers more efficiently, compromising the dynamic load inertia monitoring. On the other hand, a large value of α may result in faster convergence of the estimation algorithm to the new inertia value. However, in this case the accuracy may be compromised, as high fluctuations of the estimated parameter may result in an increase of the maximum estimation error. In other words, enhancing accuracy may deteriorate the tracking capability of the algorithm, while allowing a dynamic estimation may lead to overshoots of the estimation error. Hence, there is a trade-off between estimation accuracy and dynamic load inertia monitoring. Regardless of the smoothing method applied to remove any abnormal estimates that may occur during the estimation process, it is shown that the proposed method is able to accurately estimate and track the time-varying load inertia.

V. Conclusions

In this paper, a method to monitor the load inertia was presented. The estimation process was performed online under normal operation utilizing ambient frequency and power measurements obtained by PMUs. The load was approximated as an aggregated load model representation and the total load inertia was estimated. The LS parameter estimation method was employed to obtain the inertia value. In order to ensure estimation accuracy, the discrete low-pass filter was used for filtering the estimated values. The purpose of the smoothing process was to eliminate any possible outliers during the estimation stage, maintaining at the same time the dynamic inertia estimation capability of the algorithm. The effectiveness of the proposed estimation scheme was validated by incorporating the WECC CLM in the 39-bus test system.

A variety of load composition scenarios were tested, containing a combination of fractions of motors. In addition to the motor loads, static and electronic load fractions were also considered with adequate percentage of motors in order to contribute significantly to the system inertia. Virtual inertia from RES was not introduced in this study, but could be a possible direction for future work as a method for system operators to evaluate these ancillary services that are provided by the inverter based recourses. A time-varying load inertia scenario was presented, verifying the capability of the methodology to track both large and small load inertia fluctuations. The effect of the smoothing process was also demonstrated using different values of the smoothing constant. In this case, a trade-off between the estimation accuracy and the tracking capability of the algorithm exists. The reduced data length and the computational time that are required for the estimation process make the method suitable for near-real time applications.

References

[1] K. S. Ratnam, K. Palanisamy and G. Yang, "Future low-inertia power systems: Requirements issues and solutions—A review," *Renewable Sustain. Energy Rev*., vol. 124, May 2020.

[2] J. Fang, H. Li, Y. Tang, and F. Blaabjerg, "On the Inertia of Future More-Electronics Power Systems," *IEEE J. Emerg. Sel. Topics Power Electron*., vol. 7, no. 4, pp. 2130–2146, Oct. 2019.

[3] L. Badesa, F. Teng and G. Strbac, "Optimal Portfolio of Distinct Frequency Response Services in Low-Inertia Systems," *IEEE Trans. Power Syst.*, vol. 35, no. 6, pp. 4459-4469, Nov. 2020.

[4] GE Digital, Grid Analytics, "Effective Inertia," Accessed: April 26, 2022 [Online]. Available: https://www.ge.com/digital/sites/default/files/download_assets/effective-inertia-datasheet-ge-grid-analytics.pdf.

[5] T. Inoue, H. Taniguchi, Y. Ikeguchi, and K. Yoshida, "Estimation of power system inertia constant and capacity of spinning-reserve support generators using measured frequency transients," *IEEE Trans. Power Syst*., vol. 12, no. 1, pp. 136–143, 1997.

[6] D. P. Chassin et al., "Estimation of WECC system inertia using observed frequency transients," *IEEE Trans. Power Syst*., vol. 20, no. 2, pp. 1190–1192, 2005.

[7] D. Wilson, J. Yu, N. Al-Ashwal, B. Heimisson, and V. Terzija, "Measuring effective area inertia to determine fast-acting frequency response requirements," *Int. J. Elect. Power Energy Syst*., vol. 113, pp. 1–8, Dec. 2019.

[8] D. Yang et al., "Data-Driven Estimation of Inertia for Multiarea Interconnected Power Systems Using Dynamic Mode Decomposition," *IEEE Trans. on Ind. Inform*., vol. 17, no. 4, pp. 2686-2695, Apr. 2021.

[9] X. Cao et al., "Switching markov gaussian models for dynamic power system inertia estimation," *IEEE Trans. Power Syst*., vol. 31, no. 5, pp. 3394–3403, 2015.

[10] D. Yang et al., "Ambient-Data-Driven Modal-Identification-Based Approach to Estimate the Inertia of an Interconnected Power System," *IEEE Access*, vol. 8, pp. 118799-118807, 2020.

[11] Y. Su et al., "An Adaptive PV Frequency Control Strategy Based on Real-Time Inertia Estimation," *IEEE Trans. Smart Grid*, vol. 12, no. 3, pp. 2355-2364, May 2021.

[12] M. R. B. Tavakoli, M. Power, L. Ruttledge, D. Flynn, "Load Inertia Estimation Using White and Grey-Box Estimators for Power Systems with High Wind Penetration," *IFAC Proc*., Vol., vol. 45, no. 21, pp. 399-404, 2012.

[13] P. M. Ashton et al., ''Inertia estimation of the GB power system using synchrophasor measurements,'' *IEEE Trans. Power Syst*., vol. 30, no. 2, pp. 701–709, Mar. 2015.

[14] Y. Bian et al., "Demand Side Contributions for System Inertia in the GB Power System," *IEEE Trans. on Power Syst*., vol. 33, no. 4, pp. 3521-3530, July 2018.

[15] H. Thiesen, C. Jauch, ''Determining the Load Inertia Contribution from Different Power Consumer Groups," *Energies*, vol. 13, no. 7: 1588, 2020.

[16] R. J. Best, P. V. Brogan and D. J. Morrow, ''Power System Inertia Estimation Using HVDC Power Perturbations," *IEEE Trans. on Power Syst*., vol. 36, no. 3, pp. 1890-1899, May 2021.

[17] WECC,"WECC dynamic composite load model (CMPLDW) specifications," Technical Report, Jan. 2015.

[18] Z. Ma, Z. Wang, Y. Wang, R. Diao and D. Shi, ''Mathematical Representation of WECC Composite Load Model," *Journal of Modern Power Syst. and Clean Energy*, vol. 8, no. 5, pp. 1015-1023, Sept. 2020.

[19] P. Demetriou, M. Asprou, J. Quiros-Tortos, and E. Kyriakides, "Dynamic IEEE test systems for transient analysis," *IEEE Sys. Journal*, vol. 11, no. 4, pp. 2108–2117, 2015.